

EVOLUTION OF HOT-ROLLED TEXTURE DURING COLD ROLLING AND ANNEALING IN TI-IF STEEL

Guo Yan-hui, Zhang Xing-yao, Jing Xiao-rong

Material Engineering Department, Shanghai Institute of Technology, Shanghai, China

ABSTRACT

The evolution of hot-rolled texture during cold rolling and annealing in Ti-IF steel is comprehensively studied by X-ray diffraction analysis. Results show that an ideal γ fiber beneficial for improving deep drawability forms after annealing but only when a well-proportioned γ fiber dominates in the cold-rolled texture, which requires the formation of a strong γ fiber in the hot band.

KEY WORDS

Ti-IF steel; Hot band; texture; γ fiber

1. INTRODUCTION

Interstitial-free (IF) steels, in which the remaining carbon and nitrogen in solution are scavenged as precipitates by the addition of Ti and/or Nb, are widely used because of their excellent formability, particularly in car body panels [1, 2]. The presence of favorable texture components in IF steels results in excellent deep drawability. The strong {111} and weak {001} components parallel to the sheet plane produce good formability. The characteristics of some hot-rolled textures have been studied in literatures [3-6]. However, after hot rolling, different hot-rolled microstructures and texture arise [7-10]. The texture evolution in the whole processing system has not been discussed in detail in literature.

Hot-rolled Ti-IF steel sheets with different textures were cold rolled and annealed, and the evolution of the hot-rolled texture during cold rolling and annealing was studied by X-ray diffraction to provide a theoretical basis for obtaining the best properties.

2. EXPERIMENTAL MATERIALS AND METHODS

The experimental material was obtained from an industrial trial and its chemical composition is shown in **Table 1**.

Three hot bands with different texture were selected. The first one is hot rolled in austenite region (finish rolling temperature is 910°C). It has no γ texture. the second is hot rolled in ferrite region (finish rolling temperature is 720°C) and coiled at low temperature (440°C). It has both α and γ textures, and the third is hot rolled in ferrite region (finish rolling temperature is 760°C) and coiled at high temperature (740°C). It only has γ texture. The hot bands were cold rolled with 75% reduction to a final thickness of 1.25 mm using a two-high cold reduction mill. The cold-rolled samples were annealed in a special atmosphere furnace to simulate batch annealing.

The annealing temperature was 750 °C and the annealing time was 6 h.

For texture measurement, mid-thickness specimens were prepared by machining and paper grinding. Macroscopic textures were measured by X'Pert Pro X-ray diffractometer, and three incomplete pole figures ($\{200\}$, $\{211\}$, and $\{110\}$) were obtained. Orientation distribution functions (ODFs) were subsequently evaluated using Roe's method [11] with $l_{\max} = 16$.

3. RESULTS

3.1 The evolution of the first hot band texture

The $\varphi = 45^\circ$ ODF sections of texture are shown in **Figure 1**, which indicates that the γ fiber has not formed and the main component is the shear texture $\{110\} \langle 001 \rangle$ in the hot band texture. In addition, some weak components, $\{114\} \langle 221 \rangle$ and $\{223\} \langle 110 \rangle$, also formed. The ε -fiber showed that the intensity of the $\{110\} \langle 001 \rangle$ component was higher than 8.

Both $\{110\} \langle 001 \rangle$ and $\{114\} \langle 221 \rangle$ components disappeared, α and γ textures developed, and the intensity increased dramatically after cold rolling. The intensities of $\{111\} \langle 112 \rangle$ and $\{111\} \langle 110 \rangle$ components in the γ fiber increased after cold rolling, with $\{111\} \langle 112 \rangle$ showing slightly higher intensity.

The intensity of α texture, especially that of the $\{001\} \langle 110 \rangle$ component, decreased after annealing. The $\{111\} \langle 123 \rangle$ component increased in intensity, but $\{111\} \langle 112 \rangle$ and $\{111\} \langle 110 \rangle$ components in the γ fiber decreased in intensity.

3.2 The evolution of the second hot band texture

Figure 2 shows the $\varphi = 45^\circ$ ODF figures in hot-rolled, cold-rolled, and annealed sheets. The hot band texture includes a strong α fiber and a weak γ fiber, and the dominant components are $\{001\} \langle 110 \rangle$ to $\{223\} \langle 110 \rangle$ and $\{111\} \langle 110 \rangle$. The intensity of α texture increased, but that of γ texture changed little, after cold rolling. After annealing, γ texture intensified and α texture decreased in intensity.

3.3 The evolution of the last hot band texture

Figure 3 shows the $\varphi = 45^\circ$ ODF figures in hot-rolled, cold-rolled, and annealed sheets. After hot rolling, the most prominent texture intensity was observed along the γ fiber, and the maximum (approximately 12) was at component $\{111\} \langle 112 \rangle$. The intensities of all other textures were quite low. After cold rolling, the intensity of the γ fiber (including the $\{111\} \langle 110 \rangle$ component) decreased, whereas that of the α fiber (except the $\{111\} \langle 110 \rangle$ component) increased. The peak in the α fiber is broad and extends toward $\{223\} \langle 110 \rangle$ and $\{111\} \langle 110 \rangle$ with an intensity of 8, which indicates that grains with γ orientation rotate to α orientation, leading to high α fiber intensity. After annealing, the intensities of the γ fiber and components between $\{223\} \langle 110 \rangle$ and $\{332\} \langle 110 \rangle$ in the α fiber increased. The textures in the γ fiber stretched from $\{111\} \langle 110 \rangle$ to $\{111\} \langle 112 \rangle$ with relatively strong intensity. Orientation tended to rotate to the γ fiber, resulting in a sharp γ fiber. In the TD fiber, the highest intensity is at $\{111\} \langle 112 \rangle$, which is the most stable orientation in this fiber. The γ fiber shows that the intensity of the strongest component ($\{111\} \langle 112 \rangle$) reaches 15, which is only 1 value higher than that of $\{111\} \langle 110 \rangle$, resulting in a uniform γ fiber.

4. DISCUSSIONS

The evolution of texture is absolutely different in the three hot bands. Different hot-rolling parameters result in different hot band texture, leading to different texture evolution during cold rolling and annealing. For the first hot band, the main texture components are strong $\{110\} \langle 001 \rangle$ and weak $\{114\} \langle 221 \rangle$. Grains rotated continuously during cold rolling, which indicates increased reduction, leading to higher intensity of the α fiber. The second hot band texture comprises α and γ fibers. After cold rolling, the most prominent component transferred from $\{001\} \langle 110 \rangle$ to $\{114\} \langle 110 \rangle$, and the intensity of the γ fiber increased slightly. However, the intensity was still much weaker compared with that of the α fiber. The complete recrystallization microstructure is produced in the third hot band. The hot band texture is a recrystallization texture and not a deformation texture, which results directly from rolling. Moreover, the hot band texture characteristics are similar to those of the annealed texture in the third hot band, indicating that the third hot band can be a substitute for the conventional cold-rolled and annealed sheet. After cold rolling, the intensity of the γ fiber (including $\{111\} \langle 110 \rangle$) decreased and that of the α fiber (except $\{111\} \langle 110 \rangle$) increased, which indicates that grains with γ orientation rotate to α orientation, leading to high intensity of α fiber. The γ orientation shifted toward α orientation during cold rolling consistent with the results of a study by Inagaki [12], which indicate that crystal rotates along two paths and one of these paths is $\{110\} \langle 001 \rangle \rightarrow \{554\} \langle 225 \rangle \rightarrow \{111\} \langle 112 \rangle \rightarrow \{111\} \langle 110 \rangle \rightarrow \{223\} \langle 110 \rangle$. The γ fiber is not necessarily intensified during cold rolling and any change depends on the hot band texture. When the hot band texture comprises a strong α fiber and a weak γ fiber, the intensity of the $\{111\} \langle 110 \rangle$ component increases and the intensities of the other components in the γ fiber change little after cold rolling. When the hot band texture includes a strong γ fiber, the intensities of all components in the γ fiber decrease after cold rolling.

Textural change is also different during annealing. In the second hot band, the α fiber disappears and the intensities of $\{111\} \langle 112 \rangle$ and $\{111\} \langle 123 \rangle$ increase dramatically after annealing. Figure 2 shows that the intensity of $\{111\} \langle 123 \rangle$ increases from 2 to 11, but the intensity of $\{111\} \langle 110 \rangle$ decreases, resulting in an inhomogeneous γ fiber which shows strong anisotropy and goes against deep drawability. In the third hot band, an ideal texture for improving deep drawability is developed after annealing. Obviously, when the texture prior to annealing includes a strong α fiber and a weak γ fiber, an inhomogeneous γ fiber is formed; and when the texture prior to annealing includes a strong γ fiber, an ideal γ fiber is formed. This finding is in agreement with the results of a study by M. R. Barnett and J. J. Jonas [13,14] which showed that when rolling was finished at 70 °C and 300 °C, the hot band texture includes a partial α fiber and a complete γ fiber, and the annealed texture is an ideal γ fiber. However, when rolling was finished at 700 °C, the γ fiber does not have an obvious advantage, and the annealed texture is a γ fiber with $\{111\} \langle 112 \rangle$ in the ascent. Thus, to obtain a beneficial recrystallization texture, the γ fiber should be the most prominent texture in the un-annealed texture.

5. CONCLUSION

Hot-rolled texture has significant effect on the final texture in steel. When the hot-rolled texture contains no α and γ textures, orientation rotates along a certain way, and the cold-rolled texture consists of a strong α texture and a weak γ texture. After annealing, a non-uniform γ texture dominates, but the α texture still exists because of its high density in cold-rolled texture. When the hot-rolled texture consists of a strong α texture and a weak γ texture, the intensity of α texture increases dramatically and that of γ texture also increases slightly during cold rolling. A non-uniform γ texture with high intensity of the $\{111\} \langle 112 \rangle$ component forms after annealing. When the hot-rolled texture only contains γ texture, α texture forms and strengthens during cold

rolling, and a uniform γ texture forms after annealing. And the above results provide a theoretical basis for the industrial production.

ACKNOWLEDGEMENT

We would like to express our gratitude to all those who gave their valuable time to guide and solving doubts.

REFERENCES

- [1] Ray R K & Ghosh P, (2013) "Texture in the design of advanced steels", Transactions of the Indian Institute of Metals, Vol.66, pp.641-653.
- [2] Duggan B J, Tse Y Y, Lam G & Quadir M Z, (2011)"Deformation and recrystallization of interstitial free (IF) steel," Mater Manuf Process, Vol. 26, pp. 51-57.
- [3] Jefferson Fabrício Cardoso Lins, Hugo Ricardo Z. Sandim & Hans-Juergen Kestenbach., (2007)"Microstructural and textural characterization of a hot-rolled IFsteel," J Mater Sci, Vol. 42, PP. 6572-6577.
- [4] Gao F, Liu Z Y, Liu H T & Wang G D, (2013)"Texture evolution and formability under different hot rolling conditions in ultra purified 17%Cr ferritic stainless steels," Mater Charact, Vol.75, pp.93-100.
- [5] Han S H, Choi S H, Choi J K, Seong H J & Kim I B, (2010)"Effect of hot-rolling processing on texture and r-value of annealed dual-phase steels," Mater Sci Eng, A, Vol.527, pp.1686-1694.
- [6] Liu Y D, Zhang Y D, Ren Y, Albert T & Zuo L, (2013)"In-situ annealing study of transformation of α and γ texture of interstitial-free steel sheet by high-energy X-ray diffraction, J Iron Steel Res Int, Vol.20, pp.38-41.
- [7] Toroghinejad M R, Humphreys A O & Liu D S, (2003) "Effect of rolling temperature on the deformation and recrystallization textures of warm-rolled steels," Metall. Mater. Trans. A, Vol.34A, pp. 1163-1174.
- [8] Jeong W C, (2008) "Effect of hot-rolling temperature on microstructure and texture of an ultra-low carbon Ti-interstitial-free steel," Mater Lett, Vol.62, pp. 91-94.
- [9] Chen Y L, Su L, Zhao A M, Kuail Z, Li B H & Liu G M, (2013) "Effects of Rolling Parameters on Texture and Formability of High Strength Ultra-Low Carbon BH Steel, "J Iron Steel Res Int, Vol.20, pp. 75-81.
- [10] Guo W M, Wang Z C, Liu S & Wang X B, (2011) "Effects of finish rolling temperature on microstructure and mechanical properties of ferritic-rolled P-added high strength interstitial-free steel sheets," J Iron Steel Res Int, Vol.18, pp. 42-46.
- [11] YONG-JOON ROE R, (1965)"Description of crystallite orientation in polycrystalline materials. III general solution to pole figure inversion," J Appl Phys, Vol.36, pp.2024-2031.
- [12] Inagaki H, (1994) "Fundamental aspect of texture formation in low carbon steel. ISIJ International, Vol.34, pp. 313-321.
- [13] Barnett M R and Jonas J J, (1997) "Influence of ferrite rolling temperature in microstructure and texture in deformed low C and IF steels," ISIJ Int, Vol.37, pp. 697-705.
- [14] Barnett M R and Jonas J J, (1997) "Influence of ferrite rolling temperature on grain size and texture in annealed low C and IF steels," ISIJ Int, Vol.37, pp. 706-714.

Table 1 Chemical composition of the test steel (mass percent %).

C	Si	Mn	P	S	Ti	N	Als
0.0037	0.015	0.12	0.007	0.007	0.068	0.0028	0.034

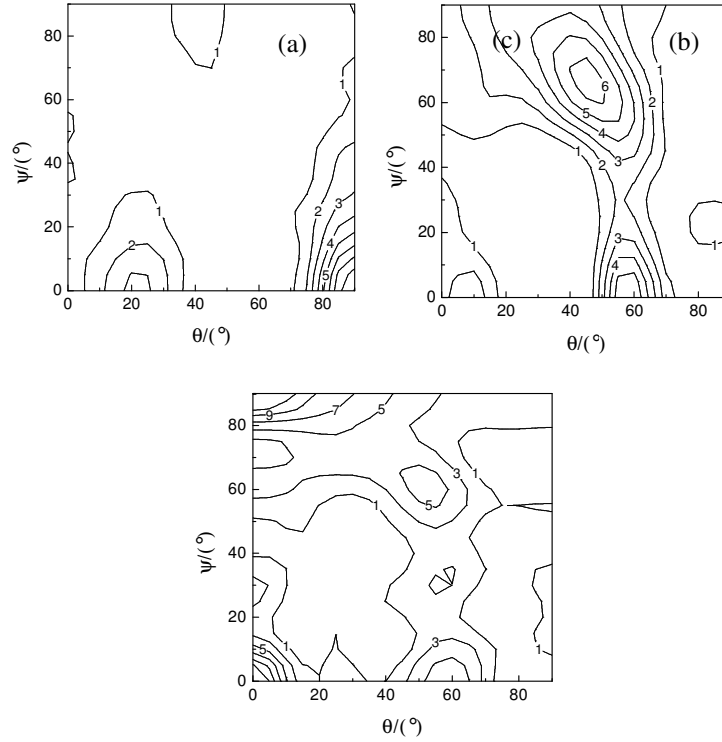


Fig. 1 $\phi = 45^\circ$ ODF sections of the first kind of Ti-IF steel.
(a) hot rolled; (b) cold rolled; (c) annealed

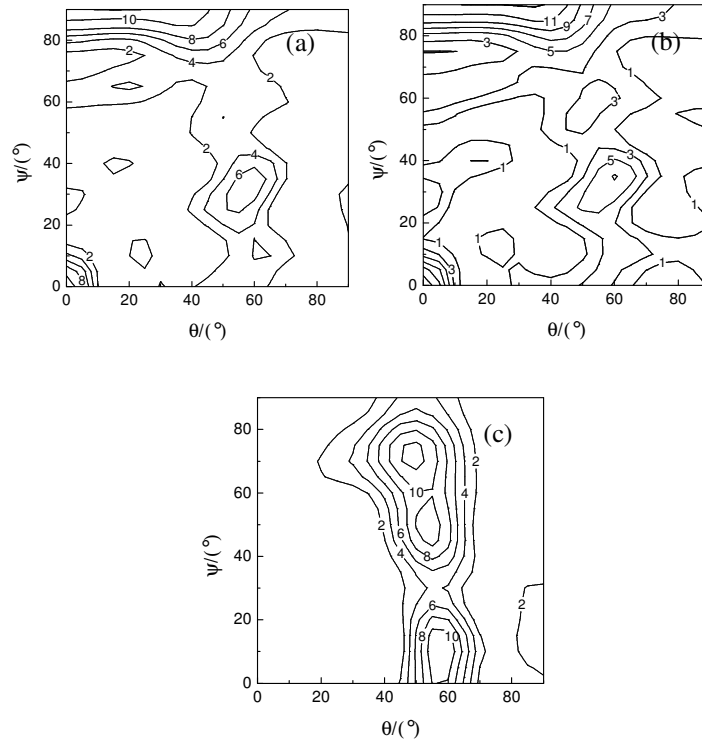
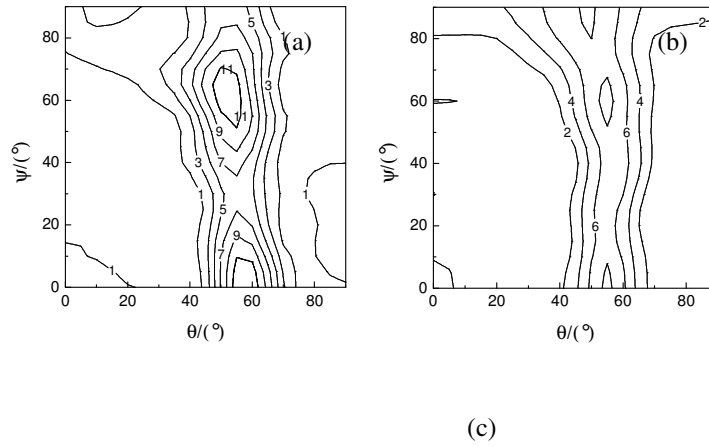


Fig.2 $\phi = 45^\circ$ ODF sections of the second kind of Ti-IF steel.
(a) hot rolled ; (b) cold rolled (c) annealed



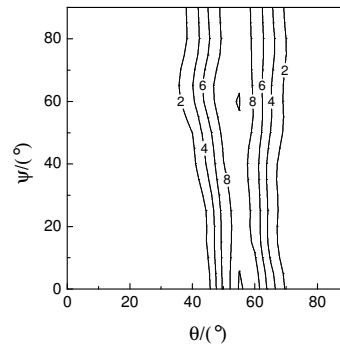


Fig. 3 $\varphi=45^\circ$ ODF sections of the third kind of Ti-IF steel.
(a) hot rolled; (b) cold rolled; (c) annealed